

A Guide to Discriminating the Rhombohedral Cell from the Face-Centred Pseudo Cubic Cell

Nobuo Ishizawa [†] and Yumi Inagaki [‡]

[†] Ceramics Research Laboratory, Nagoya Institute of Technology,
Asahigaoka 10-6-29, Tajimi, Gifu 507-0071 JAPAN

[‡] Graduate School of Nagoya Institute of Technology, Gokiso-cho, Nagoya, Aichi 466-8555

The crystal in cubic system contains four 3-fold axes with different orientations, whereas the rhombohedral modification with the face-centred pseudo cubic cell contains only one 'true' 3-fold axis. The discrimination of the 'true' 3-fold axis from the other three 'pseudo' 3-fold axes is not difficult when the rhombohedral distortion is large. However, the difficulty increases as the distortion becomes small and the cell dimensions become very close to values of 'metrically cubic'. This note first summarizes the geometrical relation among the face-centred pseudo cubic, primitive rhombohedral, and triple-hexagonal cells. Then it provides a procedure to choose the 'true' 3-fold axis, and accordingly the 'true' rhombohedral cell, from the experimentally-obtained face-centred pseudo cubic cell. In the description of this guide, a special attention has been paid for the Smart Apex II single-crystal X-ray diffractometer users.

面心擬似立方単位胞から菱面体単位胞を識別するための手引

石澤伸夫[†]・稲垣友美[‡]

[†] 名古屋工業大学セラミックス基盤工学研究センター 〒507-0071 岐阜県多治見市旭ヶ丘 10-6-29

[‡] 名古屋工業大学大学院工学研究科 〒466-8555 愛知県名古屋市昭和区御器所町

立方晶系の結晶は異なった方位をもつ四種類の三回回転軸を含むが、面心擬似立方単位胞をもつ菱面体晶系の多形における真の三回回転軸はこのうちの一種類のみである。菱面体歪みが大きい時には、真の三回回転軸を他の三種類の擬三回回転軸から識別するのは難しくない。しかし菱面体歪みが小さくなり、単位胞の寸法が数値的に立方体に極めて近くなるにつれて、識別に困難さが増す。本解説では、まず、面心擬似立方単位胞、菱面体単位胞、および三重六方単位胞の幾何学的関係を概説し、次に、実験的に得られた面心擬似立方単位胞から真の三回回転軸を見いだす方法、従って真の菱面体単位胞を見いだす方法を述べる。この手引の記述に際しては、Smart Apex II 単結晶 X 線回折計利用者のために特別な配慮を払った。

1. Introduction

The perovskite-type compounds crystallize in various symmetries. In the double perovskite defined as $A_2B'B''O_6$, where B' and B'' occupy the octahedral sites in the rock salt-type arrangement, the symmetry of the aristotype (the ideal structure with the highest symmetry) is $Fm\bar{3}m$ (for example, see Howard et al., *Acta Cryst.* B59, 463-471, 2003),

having a doubled cube edge compared with the ABO_3 perovskite aristotype ($Pm\bar{3}m$).

Among the hettotype structures exist rhombohedral modifications which are classified into two groups, one is the ' $R\bar{3}$ group' consisting of $R\bar{3}$, $R3$, $R32$, $R3m$ and $R\bar{3}m$, and the other is the ' $R\bar{3}c$ group' consisting of $R\bar{3}c$ and $R3c$. These two groups can be discriminated by the systematic reflection

conditions as will be explained in Sections 2 and 6. The rhombohedral cell can be alternatively represented by the triple-hexagonal cells in obverse or reverse settings.

The cubic crystal contains four 3-fold axes with different orientations, whereas the rhombohedral modification contains only one ‘true’ 3-fold axis. The discrimination of the ‘true’ 3-fold axis from the other three ‘pseudo’ 3-fold axes is not difficult when the rhombohedral distortion is large. However it becomes quite difficult when the distortion becomes small and the cell dimensions become very close to ‘metrically cubic’. This note first summarizes the geometrical relations among the face-centred cubic, primitive rhombohedral, and triple-hexagonal cells and then provides a practical procedure to choose the ‘true’ 3-fold axis, and accordingly the ‘true’ rhombohedral cell, from the face-centred pseudo cubic cell.

The motivation of writing this note came in the course of very difficult single-crystal structure analyses of SrTiO₃-LaAlO₃ solid solution in collaboration with Prof. H. Ohsato and his laboratory members. Most serious problem was that the crystals containing 0.5 and 20 mole% SrTiO₃ seem rhombohedral but their unit cells are close to metrically cubic. They have appreciable intensities for h - hl reflections with l =odd on the basis of the triple hexagonal obverse, suggesting that they do not belong to the R $\bar{3}c$ group, but does to either R $\bar{3}$ or Fm $\bar{3}m$. However we suffered from the difficulty in choosing the correct cell from various candidates. This was partly due to the lack in accuracy of the initial cell obtained, for example, by ‘DETERMINE UNIT CELL’ procedure of the Smart Apex II software. To overcome various difficulties in addition to this, we realized the necessities of clarifying the underlying geometrical relations and of establishing a systematic approach to identify the rhombohedral cell having almost metrically cubic dimensions. We hope this note serves to people who suffer from similar problems in different pseudo-cubic crystals.

2. The ‘obverse’ and ‘reverse’ settings for the triple-hexagonal cell

The geometrical relation of the triple-hexagonal cells in obverse and reverse settings with respect to the rhombohedral cell is shown in Fig. 2.1. The figure is essentially the same as given in Fig. 5.1.3.6 in the International Tables for Crystallography Vol. A, p84 [1]. The ‘triple’ means that there are three lattice centering points in the hexagonal cell. In this sense, the rhombohedral cell are sometimes called ‘primitive-rhombohedral’. The triple-hexagonal obverse has centering points at 0,0,0; 2/3,1/3,1/3; 1/3,2/3,2/3, whereas the triple-hexagonal reverse at 0,0,0; 1/3,2/3,1/3; 2/3,1/3,2/3. The obverse setting is recommended to use in modern crystallography. Several notes regarding the two settings are given below.

- (a) Intensities of reflections for the obverse and reverse settings satisfy the conditions below.

$$-h+k+l=3n \text{ for } hkl \text{ in obverse}$$

$$h-k+l=3n \text{ for } hkl \text{ in reverse.}$$

- (b) To check whether the current cell is recorded either obverse or reverse, we need to look at intensities of the h - hil ($i=-h-k=2h$) reflection parity groups.

$$\text{Group A: } 02\bar{2}1, 2\bar{2}01, \bar{2}021, 0\bar{2}\bar{2}\bar{1}, \bar{2}20\bar{1}, 20\bar{2}\bar{1}$$

They all satisfy the reflection condition, $-h+k+l=3n$ (obverse).

$$\text{Group B: } 02\bar{2}\bar{1}, 2\bar{2}0\bar{1}, \bar{2}02\bar{1}, 0\bar{2}21, \bar{2}201, 20\bar{2}1$$

They do not satisfy the reflection condition, $-h+k+l=3n$, whereas do the condition, $h-k+l=3n$ (reverse).

- (c) If all reflections of the parity group A have the same appreciable intensities whereas those of group B have none, then the cell setting is the obverse. Vice versa is the reverse.

- (d) To change from reverse to obverse, reverse the directions of \mathbf{a}_1 and \mathbf{a}_2 unit cell vectors in hexagonal representation:

$$\begin{pmatrix} \mathbf{a} \\ \mathbf{b} \\ \mathbf{c} \end{pmatrix}_{\text{obv}} = \begin{pmatrix} -1 & 0 & 0 \\ 0 & -1 & 0 \\ 0 & 0 & 1 \end{pmatrix} \begin{pmatrix} \mathbf{a} \\ \mathbf{b} \\ \mathbf{c} \end{pmatrix}_{\text{rev}}$$

Eq. 2.1

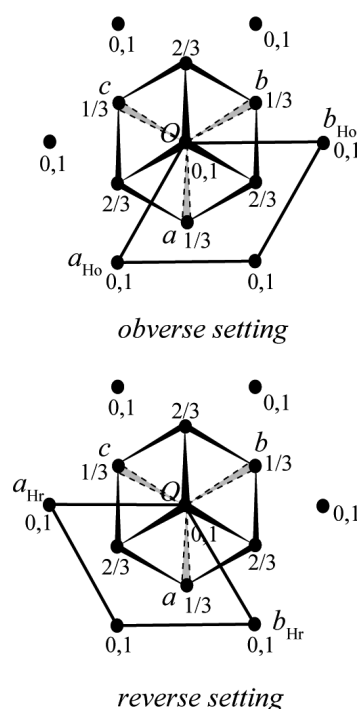


Fig. 2.1. Geometrical relation of the triple-hexagonal cells in obverse and reverse settings with respect to the rhombohedral cell

(e) The reflection parity groups A and B are used to distinguish the $\bar{R}3$ ($\bar{R}3m$, etc) and $R\bar{3}c$ groups.

$$\begin{aligned} \bar{R}3c \text{ etc: } & h+l=3n \text{ and } l=2n \text{ for } h-hl \\ \bar{R}3, R\bar{3}m \text{ etc: } & h+l=3n \text{ for } h-hl \end{aligned}$$

Since $-h+k+l=3n$ in triple-hexagonal obverse, the reflection condition for $h-hl$ are transformed into $-h+(-h)+l=-2h+l=3\{-h+(h+l)/3\}=3n$. This means that $h+l$ in small parentheses should be a multiple of 3. In other words, the condition $h+l=3n$ for $h-hl$ is not a special one, but automatically derived from the general reflection condition, $-h+k+l=3n$. Important is that the $\bar{R}3c$ group has an additional special condition, $l=2n$ for $h-hl$, whereas the $\bar{R}3$ group (incl. $\bar{R}3m$) has no special conditions other than the general one, $-h+k+l=3n$.

Note that, when the parity group A ($h-hl$, $l=\text{odd}$) has appreciable intensities, the space group is limited to the $\bar{R}3$ group (incl. $\bar{R}3m$), and cannot be the $\bar{R}3c$ group.

3. Transformation between the face centred cell and the primitive cell

3.1. Transformation matrix

Our concern lies in the transformation between the face-centred pseudo cubic (F) and the primitive rhombohedral (P) cells, but the transformation matrix between F and P is applicable to general case and not limited to the case of our concern.

$$\begin{aligned} \begin{pmatrix} \mathbf{a} \\ \mathbf{b} \\ \mathbf{c} \end{pmatrix}_F &= \begin{pmatrix} -1 & 1 & 1 \\ 1 & -1 & 1 \\ 1 & 1 & -1 \end{pmatrix} \begin{pmatrix} \mathbf{a} \\ \mathbf{b} \\ \mathbf{c} \end{pmatrix}_P \\ \begin{pmatrix} h \\ k \\ l \end{pmatrix}_F &= \begin{pmatrix} -1 & 1 & 1 \\ 1 & -1 & 1 \\ 1 & 1 & -1 \end{pmatrix} \begin{pmatrix} h \\ k \\ l \end{pmatrix}_P \end{aligned} \quad \text{Eqs. 3.1}$$

Or alternatively,

$$\begin{pmatrix} h \\ k \\ l \end{pmatrix}_P = \begin{pmatrix} 0 & 1/2 & 1/2 \\ 1/2 & 0 & 1/2 \\ 1/2 & 1/2 & 0 \end{pmatrix} \begin{pmatrix} h \\ k \\ l \end{pmatrix}_F \quad \text{Eq. 3.2}$$

Note that the transformation matrix for the real cell vectors is the same as that for reflection indices hkl .

Ex. 3-1. Conversion of several hkl 's.

$$\begin{aligned} \begin{pmatrix} h \\ h \\ l \end{pmatrix}_P &\Rightarrow \begin{pmatrix} 1 \\ 1 \\ 2h-l \end{pmatrix}_F \\ \begin{pmatrix} 1 \\ 1 \\ 1 \end{pmatrix}_P &\Rightarrow \begin{pmatrix} 1 \\ 1 \\ 1 \end{pmatrix}_F & \quad \begin{pmatrix} 2 \\ 1 \\ 1 \end{pmatrix}_P &\Rightarrow \begin{pmatrix} 1 \\ 1 \\ 3 \end{pmatrix}_F & \quad \begin{pmatrix} \bar{1} \\ \bar{1} \\ 1 \end{pmatrix}_P &\Rightarrow \begin{pmatrix} 1 \\ 1 \\ \bar{3} \end{pmatrix}_F \\ \begin{pmatrix} 0 \\ 0 \\ 2 \end{pmatrix}_P &\Rightarrow \begin{pmatrix} 2 \\ 2 \\ \bar{2} \end{pmatrix}_F & \quad \begin{pmatrix} 1 \\ 1 \\ 1 \end{pmatrix}_P &\Rightarrow \begin{pmatrix} 1 \\ 1 \\ 1 \end{pmatrix}_F \end{aligned}$$

Note that if $l=2n$ for hhl in P cell, then the converted hkl in F cell become all even. If $l=2n+1$ for hhl in P cell, then the converted hkl in F cell become all odd.

3.2. Four possible 'rhombohedral' orientations

If the true symmetry is rhombohedral, then we should identify the true 3-fold axis from four suspected 3-fold axes in pseudo FCC. In other words, we should examine four rhombohedral cells, each containing one of the four suspected 3-fold axes in FCC. The geometrical relation among four possible rhombohedral cells and the pseudo FCC cell is shown in Fig. 3.1. The filled and open circles stand for the lattice points at $z=0$ and $1/2$, respectively. The transformation from the pseudo FCC (pF) into corresponding four rhombohedral ones (R_1, R_2, R_3 and R_4) can be expressed as follows. (The first one is the same as given in Section 2.)

$$\begin{aligned} \begin{pmatrix} \mathbf{a}' \\ \mathbf{b}' \\ \mathbf{c}' \end{pmatrix}_{R_1} &= \begin{pmatrix} 0 & 1/2 & 1/2 \\ 1/2 & 0 & 1/2 \\ 1/2 & 1/2 & 0 \end{pmatrix} \begin{pmatrix} \mathbf{a} \\ \mathbf{b} \\ \mathbf{c} \end{pmatrix}_{pF} \\ \begin{pmatrix} \mathbf{a}' \\ \mathbf{b}' \\ \mathbf{c}' \end{pmatrix}_{R_2} &= \begin{pmatrix} -1/2 & 0 & 1/2 \\ 0 & 1/2 & 1/2 \\ -1/2 & 1/2 & 0 \end{pmatrix} \begin{pmatrix} \mathbf{a} \\ \mathbf{b} \\ \mathbf{c} \end{pmatrix}_{pF} \\ \begin{pmatrix} \mathbf{a}' \\ \mathbf{b}' \\ \mathbf{c}' \end{pmatrix}_{R_3} &= \begin{pmatrix} 0 & -1/2 & 1/2 \\ -1/2 & 0 & 1/2 \\ -1/2 & -1/2 & 0 \end{pmatrix} \begin{pmatrix} \mathbf{a} \\ \mathbf{b} \\ \mathbf{c} \end{pmatrix}_{pF} \\ \begin{pmatrix} \mathbf{a}' \\ \mathbf{b}' \\ \mathbf{c}' \end{pmatrix}_{R_4} &= \begin{pmatrix} 1/2 & 0 & 1/2 \\ 0 & -1/2 & 1/2 \\ 1/2 & -1/2 & 0 \end{pmatrix} \begin{pmatrix} \mathbf{a} \\ \mathbf{b} \\ \mathbf{c} \end{pmatrix}_{pF} \end{aligned} \quad \text{Eqs. 3.3}$$

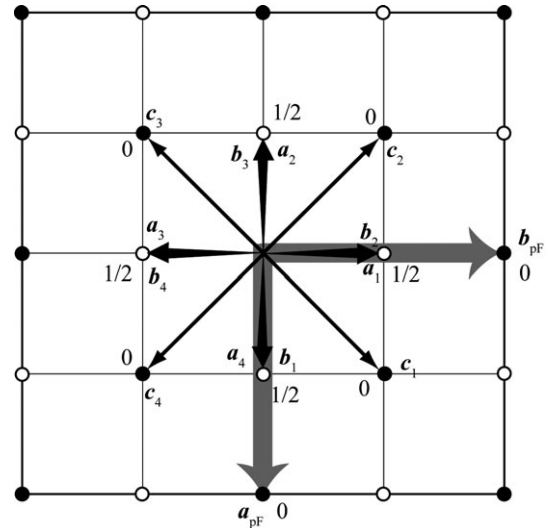


Fig. 3.1. Four possible rhombohedral cell orientations, R_i ($\mathbf{a}_i, \mathbf{b}_i, \mathbf{c}_i$) with $i=1-4$, with respect to the pseudo FCC cell ($\mathbf{a}_{pF}, \mathbf{b}_{pF}, \mathbf{c}_{pF}$). Lattice points at $z=0$ and $1/2$ of the pseudo FCC cell are denoted as solid and open circles, respectively.

The orientation relationship among the four rhombohedral cells, R_1, R_2, R_3 and R_4 , is summarized in Table 3.1 using Eqs. 3.4.

$$\begin{pmatrix} \mathbf{a} \\ \mathbf{b} \\ \mathbf{c} \end{pmatrix}_{R_i} = \mathbf{R}_{i \rightarrow j} \begin{pmatrix} \mathbf{a} \\ \mathbf{b} \\ \mathbf{c} \end{pmatrix}_{R_j}, \quad \mathbf{R}_{i \rightarrow j} = \mathbf{R}_{j \rightarrow i}^{-1}$$

Eqs. 3.4

See Table 7.1 to find similar representation for triple-hexagonal cells. Table 3.1 indicates that the four rhombohedral cells can be expressed by a single 3x3 matrix, for example, as:

$$\begin{pmatrix} \mathbf{a} \\ \mathbf{b} \\ \mathbf{c} \end{pmatrix}_{R_{i+1}} = \begin{pmatrix} 1 & 0 & -1 \\ 1 & 0 & 0 \\ 1 & -1 & 0 \end{pmatrix} \begin{pmatrix} \mathbf{a} \\ \mathbf{b} \\ \mathbf{c} \end{pmatrix}_{R_i}$$

Eq. 3.5

This equation is convenient in analyzing the four twin components in a crystal in rhombohedral form. See more details given in Section 7.2.

Note that the rotation matrices $\{(1\ 0\ -1), (1\ 0\ 0), (1\ -1\ 0)\}$ (palely hatched in Table 7.1) and $\{(0\ 1\ 0), (0\ 1\ -1), (-1\ 1\ 0)\}$ (no hatched in Table 7.1) are allowed for permuting generation of the four unit cells, while $\{(0\ 1\ -1), (1\ 0\ -1), (0\ 0\ -1)\}$ (darkly hatched in Table 7.1) is NOT. The last matrix can only convert two unit cells, for example, cells 1 and 3, or cells 2 and 4.

Table 3.1. Orientation relationship ($R_{i \rightarrow j}$) among the four possible rhombohedral cells. The subscripts i (after transformation) and j (before transformation) run from 1 through 4.

	$j=1$	$j=2$	$j=3$	$j=4$
$i=1$	-	$\begin{pmatrix} 0 & 1 & 0 \\ 0 & 1 & -1 \\ -1 & 1 & 0 \end{pmatrix}$	$\begin{pmatrix} 0 & 1 & -1 \\ 1 & 0 & -1 \\ 0 & 0 & -1 \end{pmatrix}$	$\begin{pmatrix} 1 & 0 & -1 \\ 1 & 0 & 0 \\ 1 & -1 & 0 \end{pmatrix}$
$i=2$	$\begin{pmatrix} 1 & 0 & -1 \\ 1 & 0 & 0 \\ 1 & -1 & 0 \end{pmatrix}$	-	$\begin{pmatrix} 0 & 1 & 0 \\ 0 & 1 & -1 \\ -1 & 1 & 0 \end{pmatrix}$	$\begin{pmatrix} 0 & 1 & -1 \\ 1 & 0 & -1 \\ 0 & 0 & -1 \end{pmatrix}$
$i=3$	$\begin{pmatrix} 0 & 1 & -1 \\ 1 & 0 & -1 \\ 0 & 0 & -1 \end{pmatrix}$	$\begin{pmatrix} 1 & 0 & -1 \\ 1 & 0 & 0 \\ 1 & -1 & 0 \end{pmatrix}$	-	$\begin{pmatrix} 0 & 1 & 0 \\ 0 & 1 & -1 \\ -1 & 1 & 0 \end{pmatrix}$
$i=4$	$\begin{pmatrix} 0 & 1 & 0 \\ 0 & 1 & -1 \\ -1 & 1 & 0 \end{pmatrix}$	$\begin{pmatrix} 0 & 1 & -1 \\ 1 & 0 & -1 \\ 0 & 0 & -1 \end{pmatrix}$	$\begin{pmatrix} 1 & 0 & -1 \\ 1 & 0 & 0 \\ 1 & -1 & 0 \end{pmatrix}$	-

4. Transformation between the triple-hexagonal cell in obverse setting (H) and the rhombohedral primitive cell (R)

4.1. Cell vectors and indices

$$\begin{pmatrix} \mathbf{a} \\ \mathbf{b} \\ \mathbf{c} \end{pmatrix}_R = \begin{pmatrix} 2/3 & 1/3 & 1/3 \\ -1/3 & 1/3 & 1/3 \\ -1/3 & -2/3 & 1/3 \end{pmatrix} \begin{pmatrix} \mathbf{a} \\ \mathbf{b} \\ \mathbf{c} \end{pmatrix}_H$$

$$\begin{pmatrix} h \\ k \\ l \end{pmatrix}_R = \begin{pmatrix} 2/3 & 1/3 & 1/3 \\ -1/3 & 1/3 & 1/3 \\ -1/3 & -2/3 & 1/3 \end{pmatrix} \begin{pmatrix} h \\ k \\ l \end{pmatrix}_H$$

Eqs. 4.1

Or alternatively,

$$\begin{pmatrix} h \\ k \\ l \end{pmatrix}_H = \begin{pmatrix} 1 & -1 & 0 \\ 0 & 1 & -1 \\ 1 & 1 & 1 \end{pmatrix} \begin{pmatrix} h \\ k \\ l \end{pmatrix}_R$$

Eq. 4.2

Ex. 4.1. Conversion of several hkl's.

$$\begin{pmatrix} 0 \\ 2 \\ 1 \end{pmatrix}_{\text{Hobv}} \Rightarrow \begin{pmatrix} 1 \\ 1 \\ -1 \end{pmatrix}_R \quad \begin{pmatrix} -2 \\ 0 \\ 1 \end{pmatrix}_{\text{Hobv}} \Rightarrow \begin{pmatrix} -1 \\ 1 \\ 1 \end{pmatrix}_R$$

$$\text{cf. } \begin{pmatrix} 2 \\ 0 \\ 1 \end{pmatrix}_{\text{Hrev}} \Rightarrow \begin{pmatrix} 5/3 \\ -1/3 \\ -1/3 \end{pmatrix}_R$$

The above examples tell that all the reflections allowed for the triple-hexagonal in obverse setting can be converted to the rhombohedral primitive cell with integer values, whereas part of reflections allowed for the triple-hexagonal in reverse setting result in non-integer indices. This happens because the above 201 reflection does lie on the primitive hexagonal lattice in reverse setting (Hrev), but never lie on the triple-hexagonal lattice in obverse setting (violation to the rule: $-h+k+l=3n$).

4.2. Conversion between the rhombohedral and the triple-hexagonal cell parameters

The equations for conversion are given below. In rhombohedral, $a_1=a_2=a_3(=a_R)$, $\alpha=\beta=\gamma(=\alpha)$. In hex-

agonal, $a_1=a_2(=a_H)$, $c=c_H$, $\alpha=\beta=90^\circ$, $\gamma=120^\circ$. For details, refer to Eqs. 10.40-10.43 in ‘Crystal Structures: A Working Approach’ by H. D. Megaw [2].

$$a_R = \frac{1}{3} a_H \left[3 + \left(\frac{c_H}{a_H} \right)^2 \right]^{1/2}$$

$$\alpha = 2 \sin^{-1} \frac{3}{2 \left[3 + \left(\frac{c_H}{a_H} \right)^2 \right]^{1/2}}$$

$$a_H = 2a_R \sin \frac{\alpha}{2}$$

$$\frac{c_H}{a_H} = \frac{3 \left[1 - \frac{4}{3} \sin^2 \frac{\alpha}{2} \right]^{1/2}}{2 \sin \frac{\alpha}{2}}$$

Eqs. 4.3

See Appendix 1 for the relation between the rhombohedral angle α and the hexagonal c/a ratio when c/a is close to $\sqrt{6}$ ($=2.44949$) corresponding to $\alpha=60^\circ$ (metrically FCC).

4.3. Four possible rhombohedral orientations from the experimentally-obtained ‘pseudo’ hexagonal cell

The experimentally obtained ‘triple-hexagonal’ cell could be a wrong choice (due to poor accuracy), if the ratio of the cell dimensions, c/a , is very close to $\sqrt{6}$. Figure 4.1 shows three possible alternative choices, \mathbf{R}_2 , \mathbf{R}_3 and \mathbf{R}_4 , of the ‘rhombohedral’ cell in addition to \mathbf{R}_1 which can be obtained by the normal transformation procedure given in Section 2, from experimentally-obtained triple-hexagonal cell to coincide the 3-fold axis, i.e., $[111]_R$ parallel to $[001]_H$.

Among these four candidates, the only one cell is ‘TRUE’ and the other three cells are ‘false’, if the crystal is really rhombohedral. The transformation matrices from the experimentally obtained triple-hexagonal (obverse) cell, $\mathbf{H} = (a_H, b_H, c_H)^T$, to the four possible ‘rhombohedral’ cells, $\mathbf{R}_1 = (a_1, b_1, c_1)^T$, $\mathbf{R}_2 = (a_2, b_2, c_2)^T$, $\mathbf{R}_3 = (a_3, b_3, c_3)^T$, and $\mathbf{R}_4 = (a_4, b_4, c_4)^T$ are as follows:

$$\mathbf{R}_1 = \mathbf{P}_1 \cdot \mathbf{H} = \begin{pmatrix} 2/3 & 1/3 & 1/3 \\ -1/3 & 1/3 & 1/3 \\ -1/3 & -2/3 & 1/3 \end{pmatrix} \cdot \begin{pmatrix} \mathbf{a} \\ \mathbf{b} \\ \mathbf{c} \end{pmatrix}_H$$

$$\mathbf{R}_2 = \mathbf{P}_2 \cdot \mathbf{H} = \begin{pmatrix} -1 & -1 & 0 \\ 0 & -1 & 0 \\ -1/3 & -2/3 & 1/3 \end{pmatrix} \cdot \begin{pmatrix} \mathbf{a} \\ \mathbf{b} \\ \mathbf{c} \end{pmatrix}_H$$

$$\mathbf{R}_3 = \mathbf{P}_3 \cdot \mathbf{H} = \begin{pmatrix} 1 & 0 & 0 \\ 1 & 1 & 0 \\ 2/3 & 1/3 & 1/3 \end{pmatrix} \cdot \begin{pmatrix} \mathbf{a} \\ \mathbf{b} \\ \mathbf{c} \end{pmatrix}_H$$

$$\mathbf{R}_4 = \mathbf{P}_4 \cdot \mathbf{H} = \begin{pmatrix} 0 & 1 & 0 \\ -1 & 0 & 0 \\ -1/3 & 1/3 & 1/3 \end{pmatrix} \cdot \begin{pmatrix} \mathbf{a} \\ \mathbf{b} \\ \mathbf{c} \end{pmatrix}_H$$

Eqs. 4.4

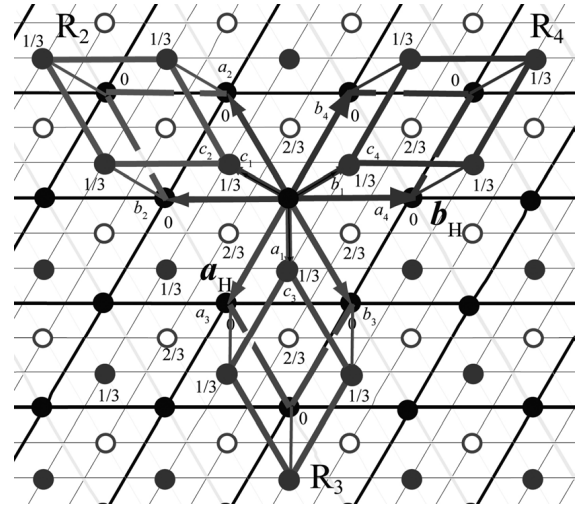


Fig. 4.1. Three pseudo primitive-‘rhombohedral’ cells, \mathbf{R}_2 , \mathbf{R}_3 and \mathbf{R}_4 , on the triple-hexagonal (obverse) lattice. The $[001]_H$ direction (c_H) is perpendicular to this paper. Lattice points of filled black circles are located at $z=0$, filled red ones at $z=1/3$, open red ones at $2/3$ ($-1/3$). The \mathbf{R}_1 cell ($\mathbf{a}_0, \mathbf{b}_0, \mathbf{c}_0$) with its 3-fold axis parallel to $[001]_H$ is omitted to avoid complexity.

4.4. Equivalent reflections for the Laue group $\bar{3}$

The reflections equivalent to triple-hexagonal and rhombohedral settings for the Laue group $\bar{3}$ are given in Tables 4.1 and 4.2.

Table 4.1. Equivalent reflections for the Laue group $\bar{3}$ in hexagonal and rhombohedral settings (a).

hexagonal hkl			rhombohedral hkl		
$h-k$	$k-l$	$h+k+l$	h	k	l
$-h-l$	$h-k$	$h+k+l$	l	h	k
$k-l$	$-h-l$	$h+k+l$	k	l	h
$-h+k$	$-k+l$	$-h-k-l$	$-h$	$-k$	$-l$
$h+l$	$-h+k$	$-h-k-l$	$-l$	$-h$	$-k$
$-k+l$	$h+k$	$-h-k-l$	$-k$	$-l$	$-h$

Table 4.2. Equivalent reflections for the Laue group $\bar{3}$ in hexagonal and rhombohedral settings (b).

hexagonal hkl			rhombohedral hkl		
h	k	l	$2h/3+k/3+l/3$	$-h/3+k/3+l/3$	$-h/3-2k/3+l/3$
$-h-k$	h	l	$-h/3-2k/3+l/3$	$2h/3+k/3+l/3$	$-h/3+k/3+l/3$
k	$-h-k$	l	$-h/3+k/3+l/3$	$-h/3-2k/3+l/3$	$2h/3+k/3+l/3$
$-h$	$-k$	$-l$	$-2h/3-k/3-l/3$	$h/3-k/3-l/3$	$h/3+2k/3-l/3$
$h+l$	$-h$	$-l$	$h/3+2k/3-l/3$	$2h/3-k/3-l/3$	$h/3-k/3-l/3$
$-k$	$h+k$	$-l$	$h/3-k/3-l/3$	$h/3+2k/3-l/3$	$-2h/3-k/3-l/3$

5. Transformation between the triple-hexagonal cell in obverse setting and the face-centred pseudo cubic cell

$$\begin{aligned} \begin{pmatrix} \mathbf{a} \\ \mathbf{b} \\ \mathbf{c} \end{pmatrix}_F &= \begin{pmatrix} -1 & 1 & 1 \\ 1 & -1 & 1 \\ 1 & 1 & -1 \end{pmatrix} \begin{pmatrix} 2/3 & 1/3 & 1/3 \\ -1/3 & 1/3 & 1/3 \\ -1/3 & -2/3 & 1/3 \end{pmatrix} \begin{pmatrix} \mathbf{a} \\ \mathbf{b} \\ \mathbf{c} \end{pmatrix}_H \\ &= \begin{pmatrix} -4/3 & -2/3 & 1/3 \\ 2/3 & -2/3 & 1/3 \\ 2/3 & 4/3 & 1/3 \end{pmatrix} \begin{pmatrix} \mathbf{a} \\ \mathbf{b} \\ \mathbf{c} \end{pmatrix}_H \\ \begin{pmatrix} h \\ k \\ l \end{pmatrix}_F &= \begin{pmatrix} -4/3 & -2/3 & 1/3 \\ 2/3 & -2/3 & 1/3 \\ 2/3 & 4/3 & 1/3 \end{pmatrix} \begin{pmatrix} h \\ k \\ l \end{pmatrix}_H \end{aligned} \quad \text{Eqs. 5.1}$$

Or alternatively,

$$\begin{aligned} \begin{pmatrix} h \\ k \\ l \end{pmatrix}_H &= \begin{pmatrix} 1 & -1 & 0 \\ 0 & 1 & -1 \\ 1 & 1 & 1 \end{pmatrix} \begin{pmatrix} 0 & 1/2 & 1/2 \\ 1/2 & 0 & 1/2 \\ 1/2 & 1/2 & 0 \end{pmatrix} \begin{pmatrix} h \\ k \\ l \end{pmatrix}_F \\ &= \begin{pmatrix} -1/2 & 1/2 & 0 \\ 0 & -1/2 & 1/2 \\ 1 & 1 & 1 \end{pmatrix} \begin{pmatrix} h \\ k \\ l \end{pmatrix}_F \end{aligned} \quad \text{Eq. 5.2}$$

Ex. 5.1. Conversion of several hkl 's.

$$\begin{pmatrix} 0 \\ 2 \\ 1 \end{pmatrix}_{\text{Hobv}} \Rightarrow \begin{pmatrix} -1 \\ -1 \\ 3 \end{pmatrix}_F \quad \text{cf.} \quad \begin{pmatrix} 0 \\ 2 \\ 1 \end{pmatrix}_{\text{Hrev}} \Rightarrow \begin{pmatrix} -5/3 \\ -5/3 \\ -7/3 \end{pmatrix}_F$$

The above examples show again that all the reflections allowed for the triple-hexagonal in obverse setting can be converted to the face-centred indices with integer values, whereas a part of reflections allowed for the triple-hexagonal in reverse setting result in non-integer. This occurs by the same reason as given in Section 4.1. The conversion of selected reflection indices are tabulated in Appendix 2.

6. Reflection conditions in the triple-hexagonal cell

6.1. Reflection conditions

In the triple-hexagonal obverse cell, the space group $R\bar{3}$ has a reflection condition of $h+l=3n$ for $h-hl$, while $R\bar{3}c$ has that of $h+l=3n$ and $l=2n$ for $h-hl$. How these conditions are modified in the transformed face-centred pseudo cubic cell, for example, represented by $Fm\bar{3}m$?

Before proceed, note that $Fm\bar{3}m$ has reflection conditions:

- (i) $h+l=2n, k+l=2n, l+h=2n$ for general hkl .
- (ii) $k=2n, l=2n$ for $0kl$,
- (iii) $h+l=2n$ for hhl ,
- (iv) $l=2n$ for $00l$.

The conditions, (ii), (iii), (iv), are derived from the general FCC condition, (i). In other words, $Fm\bar{3}m$ has no special reflection conditions other than the general FCC one, (i).

The relation between the triple-hexagonal obverse cell and the FCC cell has been derived in Eqs. 5.1. Let us check here the conditions for $h-hl$ reflections ($k=-h$).

$$\begin{aligned} \begin{pmatrix} h \\ k \\ l \end{pmatrix}_{\text{FCC}} &= \begin{pmatrix} -4/3 & -2/3 & 1/3 \\ 2/3 & -2/3 & 1/3 \\ 2/3 & 4/3 & 1/3 \end{pmatrix} \begin{pmatrix} h \\ -h \\ 1 \end{pmatrix}_{\text{Hobv}} \\ &= \begin{pmatrix} -\frac{2}{3}h + \frac{1}{3}l \\ +\frac{4}{3}h + \frac{1}{3}l \\ -\frac{2}{3}h + \frac{1}{3}l \end{pmatrix}_{\text{FCC}} \end{aligned} \quad \text{Eq. 6.2}$$

Substituting l with $3n-h$ using the equation, $h+l=3n$,

$$\begin{aligned} \begin{pmatrix} -\frac{2}{3}h + \frac{1}{3}l \\ \frac{4}{3}h + \frac{1}{3}l \\ -\frac{2}{3}h + \frac{1}{3}l \end{pmatrix}_{\text{FCC}} &= \begin{pmatrix} -\frac{2}{3}h + \frac{1}{3}(3n-h) \\ +\frac{4}{3}h + \frac{1}{3}(3n-h) \\ -\frac{2}{3}h + \frac{1}{3}(3n-h) \end{pmatrix}_{\text{FCC}} \\ &= \begin{pmatrix} -h+n \\ +h+n \\ -h+n \end{pmatrix}_{\text{FCC}} \end{aligned} \quad \text{Eq. 6.3}$$

First we consider the case, $l = \text{even}$.

$$l = 3n - h \equiv 2m \quad h = 3n - 2m$$

$$\begin{aligned} \begin{pmatrix} -h+n \\ +h+n \\ -h+n \end{pmatrix}_{\text{FCC}} &= \begin{pmatrix} -3n+2m+n \\ +3n-2m+n \\ -3n+2m+n \end{pmatrix}_{\text{FCC}} \\ &= \begin{pmatrix} -2n+2m \\ +4n-2m \\ -2n+2m \end{pmatrix}_{\text{FCC}} \\ &= 2 \begin{pmatrix} -n+m \\ +2n-m \\ -n+m \end{pmatrix}_{\text{FCC}} = \begin{pmatrix} \text{even} \\ \text{even} \\ \text{even} \end{pmatrix}_{\text{FCC}} \end{aligned} \quad \text{Eq. 6.4}$$

This indicates that the $h-hl$ ($h+l=3n$ and $l=2m$) reflections indexed on the triple-hexagonal cell are transformed into pseudo FCC with indices being all even values.

Similarly, we find that the $h-hl$ ($h+l=3n$ and $l=2m+1$) reflections indexed on the triple-hexagonal cell are transformed into pseudo FCC with indices being all odd values.

Ex. 6.1. Conversion of several hkl 's.

The h - hl reflections with $h=0$ in triple-hexagonal obverse:

$$\begin{pmatrix} -h+n \\ h+n \\ -h+n \end{pmatrix}_{\text{FCC}} \Rightarrow \begin{pmatrix} 1 \\ 1 \\ 1 \end{pmatrix}_{n=1}, \quad \begin{pmatrix} 2 \\ 2 \\ 2 \end{pmatrix}_{n=2}, \quad \begin{pmatrix} 3 \\ 3 \\ 3 \end{pmatrix}_{n=3}$$

The h - hl reflections with $h=1$ in triple-hexagonal obverse:

$$\begin{pmatrix} -1+n \\ 1+n \\ -1+n \end{pmatrix}_{\text{FCC}} \Rightarrow \begin{pmatrix} -1 \\ 1 \\ -1 \end{pmatrix}_{n=0}, \quad \begin{pmatrix} 0 \\ 2 \\ 0 \end{pmatrix}_{n=1}, \\ \begin{pmatrix} 1 \\ 3 \\ 1 \end{pmatrix}_{n=2}, \quad \begin{pmatrix} 2 \\ 4 \\ 2 \end{pmatrix}_{n=3}$$

The h - hl reflections with $h=2$ in triple-hexagonal obverse:

$$\begin{pmatrix} -2+n \\ 2+n \\ -2+n \end{pmatrix}_{\text{FCC}} \Rightarrow \begin{pmatrix} -4 \\ 0 \\ -4 \end{pmatrix}_{n=-2}, \quad \begin{pmatrix} -3 \\ 1 \\ -3 \end{pmatrix}_{n=-1}, \\ \begin{pmatrix} -2 \\ 2 \\ -2 \end{pmatrix}_{n=0}, \quad \begin{pmatrix} -1 \\ 3 \\ -1 \end{pmatrix}_{n=1}, \\ \begin{pmatrix} 0 \\ 4 \\ 0 \end{pmatrix}_{n=2}, \quad \begin{pmatrix} 1 \\ 5 \\ 1 \end{pmatrix}_{n=3}$$

Note that the h - hl ($h+l=3n$ and $l=2m+1$) reflections indexed on the triple-hexagonal cell are transformed into pseudo FCC with indices being all odd values. This never means that any hkl reflection with all odd values on the pseudo FCC cell is forbidden in the $R\bar{3}c$ group (see Section 6.2).

6.2. Procedure to discriminate $R\bar{3}$ and $R\bar{3}c$ groups

- Check hkh reflections and their permutations like hkh , khk , hkh indexed on the face-centred pseudo cubic.
- If you observe only hkh (and hkh , khk) reflections with both h and k even and no significant intensities for reflections with both h and k odd, the structure then may not be cubic and probably belongs to the $R\bar{3}c$ group. The systematic absence like this is ‘abnormal’, i.e., over-extinct for the $Fm\bar{3}m$ group.
- On the other hand, if you observe significant intensities for hkh (and hkh , khk) reflections with all odd values, then the crystal can be the $R\bar{3}c$ group. Note that no systematic absence for hkh and its permutations in FCC never exclude the possibility of $Fm\bar{3}m$.
- The discrimination between the $R\bar{3}$ and $Fm\bar{3}m$ groups based only on the systematic reflection condition is impossible. Check distortion from the cubicity, for example, deviation from 60° in the primitive rhombohedral cell, or the deviation from $\sqrt{6}$ ($=6^{1/2}$) for c/a in the triple-hexagonal cell.
- When converting the pseudo cubic cell to rhombohedral or triple-hexagonal cells, pay special attention in choosing the ‘true’ 3-fold axis because there are the other three ‘pseudo’ 3-fold

axes in the pseudo cubic cell (see Section 4.3). A mere conjecture of the ‘true’ 3-fold axis results in metrically cubic c/a or α value (see Sections 7.3-7.4).

7. General approach to discriminate ‘TRUE’ rhombohedral cell

7.1. Transformation from the pseudo cubic (pF) cell into four triple-hexagonal cells (Hobv1 ~ Hobv4)

The matrices can be obtained from Eqs. 3.3 and Eq. 4.2.

$$\begin{pmatrix} \mathbf{a} \\ \mathbf{b} \\ \mathbf{c} \end{pmatrix}_{\text{Hobv1}} = \begin{pmatrix} 1 & -1 & 0 \\ 0 & 1 & -1 \\ 1 & 1 & 1 \end{pmatrix} \begin{pmatrix} 0 & 1/2 & 1/2 \\ 1/2 & 0 & 1/2 \\ 1/2 & 1/2 & 0 \end{pmatrix} \begin{pmatrix} \mathbf{a} \\ \mathbf{b} \\ \mathbf{c} \end{pmatrix}_{\text{pF}} \\ = \begin{pmatrix} -1/2 & 1/2 & 0 \\ 0 & -1/2 & 1/2 \\ 1 & 1 & 1 \end{pmatrix} \begin{pmatrix} \mathbf{a} \\ \mathbf{b} \\ \mathbf{c} \end{pmatrix}_{\text{pF}}$$

$$\begin{pmatrix} \mathbf{a} \\ \mathbf{b} \\ \mathbf{c} \end{pmatrix}_{\text{Hobv2}} = \begin{pmatrix} 1 & -1 & 0 \\ 0 & 1 & -1 \\ 1 & 1 & 1 \end{pmatrix} \begin{pmatrix} -1/2 & 0 & 1/2 \\ 0 & 1/2 & 1/2 \\ -1/2 & 1/2 & 0 \end{pmatrix} \begin{pmatrix} \mathbf{a} \\ \mathbf{b} \\ \mathbf{c} \end{pmatrix}_{\text{pF}} \\ = \begin{pmatrix} -1/2 & -1/2 & 0 \\ 1/2 & 0 & 1/2 \\ -1 & 1 & 1 \end{pmatrix} \begin{pmatrix} \mathbf{a} \\ \mathbf{b} \\ \mathbf{c} \end{pmatrix}_{\text{pF}}$$

$$\begin{pmatrix} \mathbf{a} \\ \mathbf{b} \\ \mathbf{c} \end{pmatrix}_{\text{Hobv3}} = \begin{pmatrix} 1 & -1 & 0 \\ 0 & 1 & -1 \\ 1 & 1 & 1 \end{pmatrix} \begin{pmatrix} 0 & -1/2 & 1/2 \\ -1/2 & 0 & 1/2 \\ -1/2 & -1/2 & 0 \end{pmatrix} \begin{pmatrix} \mathbf{a} \\ \mathbf{b} \\ \mathbf{c} \end{pmatrix}_{\text{pF}} \\ = \begin{pmatrix} 1/2 & -1/2 & 0 \\ 0 & 1/2 & 1/2 \\ -1 & -1 & 1 \end{pmatrix} \begin{pmatrix} \mathbf{a} \\ \mathbf{b} \\ \mathbf{c} \end{pmatrix}_{\text{pF}}$$

$$\begin{pmatrix} \mathbf{a} \\ \mathbf{b} \\ \mathbf{c} \end{pmatrix}_{\text{Hobv4}} = \begin{pmatrix} 1 & -1 & 0 \\ 0 & 1 & -1 \\ 1 & 1 & 1 \end{pmatrix} \begin{pmatrix} 1/2 & 0 & 1/2 \\ 0 & -1/2 & 1/2 \\ 1/2 & -1/2 & 0 \end{pmatrix} \begin{pmatrix} \mathbf{a} \\ \mathbf{b} \\ \mathbf{c} \end{pmatrix}_{\text{pF}} \\ = \begin{pmatrix} 1/2 & 1/2 & 0 \\ -1/2 & 0 & 1/2 \\ 1 & -1 & 1 \end{pmatrix} \begin{pmatrix} \mathbf{a} \\ \mathbf{b} \\ \mathbf{c} \end{pmatrix}_{\text{pF}}$$

Eqs. 7.1

These four transformations are important in the discrimination of the true rhombohedral cell from the pseudo FCC when the c/a ratio is close to $\sqrt{6}$ in triple-hexagonal, or α is close to 60° in primitive rhombohedral. To convert a candidate of triple hexagonal cell, for example, Hobv₁ to the other candidates, i.e., Hobv₂, Hobv₃ and Hobv₄, see Section 7.2.

7.2. Geometrical relationship among the four triple-hexagonal cells

The orientation relationship among the four triple-hexagonal cells, Hobv₁, Hobv₂, Hobv₃ and Hobv₄, is summarized in Table 7.1, using Eqs. 7.2.

$$\begin{pmatrix} \mathbf{a} \\ \mathbf{b} \\ \mathbf{c} \end{pmatrix}_{\text{Hobv(i)}} = \mathbf{R}_{i \rightarrow j} \begin{pmatrix} \mathbf{a} \\ \mathbf{b} \\ \mathbf{c} \end{pmatrix}_{\text{Hobv(j)}}, \quad \mathbf{R}_{i \rightarrow j} = \mathbf{R}_{j \rightarrow i}^{-1}$$

Eqs. 7.2

Table 7.1 indicates that the four twin components can be represented iteratively as follows:

$$\begin{pmatrix} \mathbf{a} \\ \mathbf{b} \\ \mathbf{c} \end{pmatrix}_{\text{Hobv}(i+1)} = \begin{pmatrix} 1/3 & 2/3 & -1/3 \\ -1/3 & 1/3 & 1/3 \\ 8/3 & 4/3 & 1/3 \end{pmatrix} \begin{pmatrix} \mathbf{a} \\ \mathbf{b} \\ \mathbf{c} \end{pmatrix}_{\text{Hobv}(i)} \quad \text{Eq. 7.3}$$

Or using the ‘i’-times repeated multiplication of the matrix,

$$\begin{pmatrix} \mathbf{a} \\ \mathbf{b} \\ \mathbf{c} \end{pmatrix}_{\text{Hobv}(i)} = \begin{pmatrix} 1/3 & 2/3 & -1/3 \\ -1/3 & 1/3 & 1/3 \\ 8/3 & 4/3 & 1/3 \end{pmatrix}^i \begin{pmatrix} \mathbf{a} \\ \mathbf{b} \\ \mathbf{c} \end{pmatrix}_{\text{Hobv}(1)} \quad \text{Eq. 7.4}$$

These expressions are useful for twin analysis because the four twin components can be represented by iterating a single transformation matrix up to four times. If you are the SHELX user and want to determine the amounts of these four possible twin components in a crystal, you may add the following lines, for example, in the instruction file of .ins as:

```
TWIN 0.3333 0.6667 -0.3333 -0.3333 0.3333
      0.3333 2.6667 1.3333 0.3333 4
BASF k2 k3 k4
```

Note that the TWIN line may truncate if you use too many digits for the values. The rotation matrix $\begin{bmatrix} 1/3 & 2/3 & -1/3 \\ 2/3 & -1/3 & -1/3 & 1/3 & 1/3 & 8/3 & 4/3 & 1/3 \end{bmatrix}$ is then applied 3(=4-1) times to generate the indices of twin components from the input reflection indices which apply to the first component. The scale factors k_m for the twin components are calculated from :

$$F_c^2 = (\text{osf})^2 \sum_{m=1}^n k_m F_{c_m}^2 \quad \text{Eq. 7.5}$$

In the above equation, ‘osf’ is the overall scale factor, and $n=4$. Initial scale factors, k_2 , k_3 , and k_4 for the twin components for variants 2, 3 and 4 are necessary as inputs ($0 \leq k_m \leq 1$). The scale factor k_1 for the twin component 1 is calculated from the equation:

$$k_1 = 1 - \sum_{m=2}^n k_m \quad \text{Eq. 7.6}$$

Note that the rotation matrices $\{(1/3 \ 2/3 \ -1/3), (-1/3 \ 1/3 \ 1/3), (8/3 \ 4/3 \ 1/3)\}$ and $\{(-1/3 \ -2/3 \ 1/3), (1 \ 1 \ 0), (-4/3 \ 4/3 \ 1/3)\}$ in Table 7.1 are allowed for permutation in generating four twin components, while $\{(-1 \ 0 \ 0), (2/3 \ 1/3 \ 1/3), (4/3 \ 8/3 \ -1/3)\}$ is NOT. The last matrix can convert between only two twin components, for example, components between 1 and 3, or those between 2 and 4.

Table 7.1. Orientation relationship ($\mathbf{R}_{i \rightarrow j}$) among the four possible triple-hexagonal cells. The subscripts i (after transformation) and j (before transformation) run from 1 through 4.

	$j=1$ (Hobv ₁)	$j=2$ (Hobv ₂)	$j=3$ (Hobv ₃)	$j=4$ (Hobv ₄)
$i=1$ (Hobv ₁)	-	$\begin{pmatrix} -1/3 & -2/3 & 1/3 \\ 1 & 1 & 0 \\ -4/3 & 4/3 & 1/3 \end{pmatrix}$	$\begin{pmatrix} -1 & 0 & 0 \\ 2/3 & 1/3 & 1/3 \\ 4/3 & 8/3 & -1/3 \end{pmatrix}$	$\begin{pmatrix} 1/3 & 2/3 & -1/3 \\ -1/3 & 1/3 & 1/3 \\ 8/3 & 4/3 & 1/3 \end{pmatrix}$
$i=2$ (Hobv ₂)	$\begin{pmatrix} 1/3 & 2/3 & -1/3 \\ -1/3 & 1/3 & 1/3 \\ 8/3 & 4/3 & 1/3 \end{pmatrix}$	-	$\begin{pmatrix} -1/3 & -2/3 & 1/3 \\ 1 & 1 & 0 \\ -4/3 & 4/3 & 1/3 \end{pmatrix}$	$\begin{pmatrix} -1 & 0 & 0 \\ 2/3 & 1/3 & 1/3 \\ 4/3 & 8/3 & -1/3 \end{pmatrix}$
$i=3$ (Hobv ₃)	$\begin{pmatrix} -1 & 0 & 0 \\ 2/3 & 1/3 & 1/3 \\ 4/3 & 8/3 & -1/3 \end{pmatrix}$	$\begin{pmatrix} 1/3 & 2/3 & -1/3 \\ -1/3 & 1/3 & 1/3 \\ 8/3 & 4/3 & 1/3 \end{pmatrix}$	-	$\begin{pmatrix} -1/3 & -2/3 & 1/3 \\ 1 & 1 & 0 \\ -4/3 & 4/3 & 1/3 \end{pmatrix}$
$i=4$ (Hobv ₄)	$\begin{pmatrix} -1/3 & -2/3 & 1/3 \\ 1 & 1 & 0 \\ -4/3 & 4/3 & 1/3 \end{pmatrix}$	$\begin{pmatrix} -1 & 0 & 0 \\ 2/3 & 1/3 & 1/3 \\ 4/3 & 8/3 & -1/3 \end{pmatrix}$	$\begin{pmatrix} 1/3 & 2/3 & -1/3 \\ -1/3 & 1/3 & 1/3 \\ 8/3 & 4/3 & 1/3 \end{pmatrix}$	-

7.3. Practices -Case 1-

It would be a good idea to get the knack of successful identification through practices. Let us start from a 'TRUE' rhombohedral cell with $a=5.400 \text{ \AA}$, $\alpha=60.02^\circ$. This is a cell likely to occur in the $\text{SrTiO}_3\text{-LaAlO}_3$ solid solution system, especially in the crystal containing 20 mole% SrTiO_3 . Table 7.2 shows how the cell parameters vary depending on the cells under assumption.

The primitive rhombohedral cell (R) can be converted to a 'TRUE' triple-hexagonal cell (Hobv1) and a 'TRUE' pseudo FCC cell (pF) using transformations given in Eqs. 4.1 and Eqs. 5.1, respectively. Using Eqs. 7.2 and 7.3, the triple-hexagonal cell (Hobv1) can be transformed into Hobv₂, Hobv₃ and Hobv₄. Several interaxial angles of these 'FALSE' hexagonal cells have small deviations of $0.01\text{-}0.02^\circ$ from ideal values. In addition, there is a small difference of less than 0.002 \AA in a and b lengths.

Table 7.2. Various cell parameters obtained for the Case 1. See text for the cell abbreviation.

cell	a	b	c	α	β	γ	comment
R	5.4000	5.4000	5.4000	60.020	60.020	60.020	TRUE
pF	7.6379	7.6379	7.6379	90.017	90.017	90.017	TRUE
Hobv ₁	5.4016	5.4016	13.2252	90.000	90.000	120.000	TRUE
Hobv ₂	5.3996	5.3998	13.2305	90.013	89.984	119.979	FALSE
Hobv ₃	5.4016	5.3999	13.2303	89.984	90.000	120.010	FALSE
Hobv ₄	5.3998	5.4016	13.2303	90.000	90.013	120.008	FALSE

Table 7.3. Various cell parameters obtained for the Case 2. See text for the cell abbreviation.

cell	a	b	c	α	β	γ	comment
Hobv ₁	5.3998	5.4016	13.2303	90.000	90.013	120.008	FALSE
R ₁	5.4000	5.4015	5.4016	60.001	59.991	59.989	FALSE
pF ₁	7.6377	7.6378	7.6380	90.017	89.985	89.981	FALSE
Hobv ₂	5.4012	5.4013	13.2251	89.997	89.998	119.997	TRUE
R ₂	5.4001	5.3998	5.3997	60.019	60.020	60.015	TRUE
pF ₂	7.6373	7.6374	7.6381	90.013	90.018	90.016	TRUE
Hobv ₃	5.3998	5.3999	13.2305	90.011	89.986	119.980	FALSE
R ₃	5.4016	5.4000	5.4014	59.990	60.000	59.988	FALSE
pF ₃	7.6376	7.6376	7.6380	89.982	90.016	89.983	FALSE
Hobv ₄	5.4013	5.4000	13.2300	89.983	90.000	120.008	FALSE
R ₄	5.4015	5.4015	5.3997	59.993	59.993	59.998	FALSE
pF ₄	7.6375	7.6375	7.6382	89.984	89.984	90.017	FALSE

7.4. Practices -Case 2-

Let us consider another case (Case 2). Suppose we have obtained experimentally the data of Hobv₁ in Table 7.3. According to the procedure given in 7.2, we can obtain the other three candidates of Hobv₂, Hobv₃ and Hobv₄ as listed in Table 7.3, with their corresponding primitive rhombohedral (R_n) and pseudo cubic (pF_n) cell dimensions, $n=1\sim 4$. Which is the 'TRUE' one?

For the first time you feel a difficulty in answering to this question because none of the four candidates have the exact geometrical relations required for the ideal cells. However, by looking into data closely,

you can find some characteristic tendencies. This appears most typically in the primitive rhombohedral cell. The answer is that the 'TRUE' cell is Hobv₂. Supporting evidences are given below.

- (a) The 'TRUE' primitive rhombohedral cell has the largest (and mostly equal) deviations from 60° for the three interaxial angles. FALSE cells have usually plus-and-minus mixed deviations from 60° due to its distorted cell nature. In addition, the deviations from 60° in 'FALSE' cells are usually smaller by an order of magnitude and come closer

to a cubic cell in average (recall $\alpha_R=60^\circ$ for the metrically FCC cell).

- (b) The cell lengths of the 'TRUE' primitive rhombohedral have the smallest deviation among them. In Case 2, the deviation for R_2 is less than 0.0004 Å, while R_1 , R_3 and R_4 are 0.0016, 0.0016, 0.0018 Å, respectively. The deviation in R_2 is one figure small compared with the 'FALSE' cells.

If you look into the cell dimensions in the pseudo cubic setting, you will find more information to tell about the discrimination of the 'TRUE' cell. An important thing is that even a 'TRUE' cell does not have the 'exact' geometrical relations in experiments. This, of course, never means that it is useless to improve accuracy. On the contrary, we should try to enhance the quality of experiment to improve accuracy as much as possible. After that, find most distorted cell from the candidates. The distortion is a measure of departure from cubicity. The FALSE cells tend to assume cubicity in a sort of the averaged way. If the distortions occur most systematically and prominently in only one candidate cell, then the cell is most plausibly the right answer.

Finally we would like to reveal that the numerical data used in Case 2 are essentially made from those in Case 1. Actually we just picked up the $Hobv_4$ data of Case 1, assumed that they are obtained experimentally, and put them as $Hobv_1$ in Case 2. The recalculation from this new $Hobv_1$ to $Hobv_2$, $Hobv_3$ and $Hobv_4$ brought slightly different values from those listed in Case 1, probably due to the termination errors during numerical operations, for example, an input of 0.3333 instead of 1/3. As a result, the 'TRUE' answer lost its exactness slightly, which served, in turn, for usage as a 'practical' example.

8. A convenient technique of discrimination using the Smart Apex II software

- (a) Collect data assuming any temporary cell found in the process 'DETERMINE UNIT CELL'. Assumption of a primitive cell with the same cell volume as that of the 'true' cell could be recommended for running 'STRATEGY'. Collect as many frames as possible up to the highest diffraction angle available for the time you are allowed to use the machine. For inorganic crystals the ω and ϕ scan widths less than 0.3° are recommended when the crystal-to-detector distance is approximately 60 mm. If necessary, increase the total scan range.
- (b) After data collection, run again 'DETERMINE UNIT CELL', using much more frames than the default values if the starting cell is supposed to contain large errors. A series of successive runs (a set of frames) with lower diffraction angles is recommended. The number of successive runs can be 3 to 5, and the number of frames in a single run can be 100-200, for example. This will take a slightly longer time but would give much better initial cell parameters than the previous results obtained in a).
- (c) If you get a plausible cell like triple-hexagonal, primitive rhombohedral or face-centred pseudo

cubic cells, check carefully the deviation of cell parameters from their 'ideal' values, for example, deviation of c/a ratio from $\sqrt{6}$ and angular deviations from 90° and 120° for the triple-hexagonal cell. Check three α angles of the primitive rhombohedral cell using 'BRAVAIS'. If necessary, use Eqs. 4.3 in calculating α . They should be deviated from 60° with the equal amount, for example, 60.03° , 60.03° , 60.03° . If the α values are scattered in various ways, like, 59.96, 60.03, 60.02, the cell is probably FALSE. But never mind and proceed.

- (d) Go to the procedure 'INTEGRATE' and click 'REFINEMENT OPTION'. Enter 200 (number of frames), for example, instead of 50 (default) in the 'FREQUENCY (Images)' in the 'Periodic Refinement' panel. The periodic refinement of various system parameters at longer intervals (i.e., using more frames) is important if the crystal contains a small number of reflections per frame. The groups of frames (RUNS) with low numbers are usually collected at relatively high angles (see STRATEGY). These frames are less crowded with weak diffraction spots. These peaks are highly possible to go missing in the 'INTEGRATE' procedure if the orientation matrix (UB matrix) is inaccurate. Therefore, the periodic refinement using a small number of frames like default value is dangerous for many inorganic crystals and may introduce serious errors in the system parameters to be refined. Do not forget to set the d (Å) limit in top right corner of the window panel to an appropriate value. It is recommended to choose 'TRICLINIC' for the option 'CONSTRAINT METRIC SYSTEM' in both 'PERIODIC REFINEMENT' and 'GLOBAL REFINEMENT' panels. Be careful in using the default crystal system for 'CONSTRAINT METRIC SYSTEM', because the default is the one previously determined in the 'DETERMINE UNIT CELL' procedure.
- (e) After 'INTEGRATE', check carefully the created file 'XXX_0m.ls'. You find three sets of the refined cell parameters in the very last part of the file.
- (f) Go to 'EXAMINE DATA' and run 'XPREP' (IMPORTANT)
- (g) The first thing to do on entering 'EXAMINE DATA', is to specify the p4p file and raw data file you are going to use. They are usually 'XXX_0m.p4p' and 'XXX_0m.raw' in the working directory. You will find on the screen the initial check results about the 'Lattice Exceptions'. Look carefully into the O (obverse) and R (reverse) exceptions when you use the triple-hexagonal cell. If you find many exceptions in both columns, it never be triple-hexagonal (though the possibility of twinning of triple-hexagonal cells still remains). Whichever is the cell obverse or reverse, just keep it in mind and accept the recommendation for this time. There is no need to transform the cell from reverse to obverse (see step (i) for the reason). Then 'XPREP' shows various options to proceed.
- (h) Choose 'UNIT CELL TRANSFORMATION (U)' and 'FIND NIGGLI REDUCED CELLS (N)'. This routine finds reduced cells from multi-centred cells, for

example, triple-hexagonal or face-centred pseudo cubic by the Niggli method^[3]. If your original cell is triple-hexagonal, then you will find a reduced primitive rhombohedral Niggli cell, which indicates the direction of the ‘true’ 3-fold axis in high probability. Check three α angles of the primitive rhombohedral cell shown in the results carefully. They may be deviated from 60° with approximately the equal amount, for example, 60.03 , 60.03 , 60.04° (Congratulation!). Now your current cell is primitive rhombohedral.

- (i) If you prefer to transform once again from the primitive rhombohedral to triple-hexagonal in obverse setting, type ‘U’ to run ‘UNIT CELL TRANSFORMATION (U)’. Enter transformation matrix like ‘1 -1 0 0 1 -1 1 1 1’, as given in Section 4.1, Eq. 4.2. This will convert the current primitive rhombohedral cell to triple-hexagonal cell in obverse. Even though the original cell was reverse, your latest current cell in the top panel is now obverse after the procedures of (N) and (U) as above. The procedure described in the steps (h) and (i) is the key of this technical note.
- (j) Go back to the ‘XPREP’ main menu and do necessary things to prepare .ins and .hkl files using the options:
 ‘ENTER SPACE GROUP (S)’ to enter $R\bar{3}$ etc
 ‘DEFINE UNIT CELL CONTENTS (C)’ to enter Z value
 ‘ABSORPTION CORRECTOOPN etc. (A)’ for absorption correction
 ‘SETUP SHELX FILES (S)’ to create XXXX.hkl (any file name with a suffix of .hkl).
- (k) Finally, if you want to make consistent various files created during this process, especially in order to keep the consistency of reflection indices, precession images, crystal faces for absorption, I recommend to start over the whole processes maybe from INTEGRATE and PRECESSION, importing the latest .p4p to the system.

The steps from (g) through (k) will solve most difficult and intrinsic problems associated with the identification of the real symmetry of the face-centred pseudo cubic cells.

9. A practical guide to finding ‘TRUE’ rhombohedral cell from the UB matrix

9.1. UB and G matrices

The orientation of the crystal on the diffractometer is expressed by the matrix \mathbf{UB} where the matrix \mathbf{B} is defined as:

$$\mathbf{B} = \begin{pmatrix} a^* & b^* \cos \gamma^* & c^* \cos \beta^* \\ 0 & b^* \sin \gamma^* & -c^* \sin \beta^* \cos \alpha \\ 0 & 0 & 1/c \end{pmatrix} \quad \text{Eq. 9.1}$$

Lattice vectors are obtained from of the G matrix which is the inverse matrix of a product of \mathbf{UB} and its transposition, \mathbf{UB}^T :

$$\begin{aligned} \mathbf{G} &= \{(\mathbf{UB})^T \cdot \mathbf{UB}\}^{-1} = (\mathbf{B}^T \mathbf{U}^T \mathbf{UB})^{-1} = (\mathbf{B}^T \mathbf{B})^{-1} \\ &= \begin{pmatrix} \mathbf{aa} & \mathbf{ab} & \mathbf{ac} \\ \mathbf{ba} & \mathbf{bb} & \mathbf{bc} \\ \mathbf{ca} & \mathbf{cb} & \mathbf{cc} \end{pmatrix} \\ &= \begin{pmatrix} a^2 & ab \cos \gamma & ac \cos \beta \\ ab \cos \gamma & b^2 & bc \cos \alpha \\ ac \cos \beta & bc \cos \alpha & c^2 \end{pmatrix} \end{aligned} \quad \text{Eq. 9.2}$$

Suppose that cell vectors are transformed by the 3x3 matrix \mathbf{P} as:

$$\begin{pmatrix} \mathbf{a}' \\ \mathbf{b}' \\ \mathbf{c}' \end{pmatrix} = \mathbf{P} \cdot \begin{pmatrix} \mathbf{a} \\ \mathbf{b} \\ \mathbf{c} \end{pmatrix} \quad \text{Eq. 9.3}$$

Then the relation between the \mathbf{G} and \mathbf{G}' matrices of the old and new cell vectors, respectively, can be written as:

$$\begin{aligned} \mathbf{G} &= \mathbf{P}^{-1} \begin{pmatrix} \mathbf{a}' \\ \mathbf{b}' \\ \mathbf{c}' \end{pmatrix} \left\{ \mathbf{P}^{-1} \begin{pmatrix} \mathbf{a}' \\ \mathbf{b}' \\ \mathbf{c}' \end{pmatrix} \right\}^T \\ &= \mathbf{P}^{-1} \begin{pmatrix} \mathbf{a}' \\ \mathbf{b}' \\ \mathbf{c}' \end{pmatrix} (\mathbf{a}' \quad \mathbf{b}' \quad \mathbf{c}') \cdot (\mathbf{P}^{-1})^T \\ &= \mathbf{P}^{-1} \mathbf{G}' (\mathbf{P}^{-1})^T \end{aligned} \quad \text{Eq. 9.4}$$

Applying \mathbf{P} from left and \mathbf{P}^T from right to the both sides of Eq. 9.4:

$$\begin{aligned} \mathbf{PGP}^T &= \mathbf{PP}^{-1} \mathbf{G}' (\mathbf{P}^{-1})^T \mathbf{P}^T = \mathbf{PP}^{-1} \mathbf{G}' (\mathbf{PP}^{-1})^T \\ &= \mathbf{EG}' (\mathbf{E})^T \\ \therefore \mathbf{G}' &= \mathbf{PGP}^T \end{aligned} \quad \text{Eqs. 9.5}$$

9.2. Four possible rhombohedral cells from the experimentally-obtained triple-hexagonal cell

The experimentally obtained ‘triple-hexagonal’ cell could have been obtained based on a wrong choice (due to poor accuracy), if the ratio of the cell dimensions, c/a , is very close to $\sqrt{6}$. As mentioned in Section 4.3, there are four possible ‘rhombohedral’ cells. Among these four candidates, the only one cell is ‘TRUE’ and the other three cells are ‘FALSE’, if the crystal is really rhombohedral. The transformation matrices from the experimentally obtained triple-hexagonal (obverse) cell, $\mathbf{H} = (\mathbf{a}_H, \mathbf{b}_H, \mathbf{c}_H)^T$, to these four possible rhombohedral cells, $\mathbf{R}_1 = (\mathbf{a}_1, \mathbf{b}_1, \mathbf{c}_1)^T$, $\mathbf{R}_2 = (\mathbf{a}_2, \mathbf{b}_2, \mathbf{c}_2)^T$, $\mathbf{R}_3 = (\mathbf{a}_3, \mathbf{b}_3, \mathbf{c}_3)^T$, and $\mathbf{R}_4 = (\mathbf{a}_4, \mathbf{b}_4, \mathbf{c}_4)^T$ are as follows:

$$\mathbf{R}_1 = \mathbf{P}_1\mathbf{H} = \begin{pmatrix} 2/3 & 1/3 & 1/3 \\ -1/3 & 1/3 & 1/3 \\ -1/3 & -2/3 & 1/3 \end{pmatrix} \begin{pmatrix} \mathbf{a} \\ \mathbf{b} \\ \mathbf{c} \end{pmatrix}_H$$

$$\mathbf{R}_2 = \mathbf{P}_2\mathbf{H} = \begin{pmatrix} -1 & -1 & 0 \\ 0 & -1 & 0 \\ -1/3 & -2/3 & 1/3 \end{pmatrix} \begin{pmatrix} \mathbf{a} \\ \mathbf{b} \\ \mathbf{c} \end{pmatrix}_H$$

$$\mathbf{R}_3 = \mathbf{P}_3\mathbf{H} = \begin{pmatrix} 1 & 0 & 0 \\ 1 & 1 & 0 \\ 2/3 & 1/3 & 1/3 \end{pmatrix} \begin{pmatrix} \mathbf{a} \\ \mathbf{b} \\ \mathbf{c} \end{pmatrix}_H$$

$$\mathbf{R}_4 = \mathbf{P}_4\mathbf{H} = \begin{pmatrix} 0 & 1 & 0 \\ -1 & 0 & 0 \\ -1/3 & 1/3 & 1/3 \end{pmatrix} \begin{pmatrix} \mathbf{a} \\ \mathbf{b} \\ \mathbf{c} \end{pmatrix}_H$$

Eqs. 9.6

The converted cell dimensions can be obtained by the equation, $\mathbf{G}' = \mathbf{P}\mathbf{G}\mathbf{P}^T$, where \mathbf{P} is substituted by \mathbf{P}_1 , \mathbf{P}_2 , \mathbf{P}_3 or \mathbf{P}_4 . These cell dimensions should be carefully examined in the light of metric constraints for rhombohedron, $a=b=c$, $\alpha=\beta=\gamma$. For this evaluation, you have to use an accurate \mathbf{UB} matrix, and thus \mathbf{G} , because the small metrical offsets from the ideal values have of vital importance. On Smart Apex II software, it is better to use 'UNCONSTRAINED' setting parameter (\mathbf{UB} matrix). You can find it in the output file, XXX_ls, which is created after the INTEGRATE procedure.

9.3. Example

9.3.1. Direct conversion from the pseudo hexagonal to rhombohedral candidates

Below is an example obtained from the single crystal synchrotron experiment at BL14A using a 0.5mol%SrTiO₃-99.5mol%LaAlO₃ mixed crystal (ST05_2) in June 5, 2008. The wavelength of X-rays is 0.671710Å. The crystal was ground into spherical shape with 70-80 μm in diameter. The orientation matrix \mathbf{UB} of the initial hexagonal cell was refined as below:

$$\mathbf{UB} = \begin{pmatrix} 0.1291097 & -0.0752697 & 0.0200698 \\ 0.1697295 & 0.1815203 & -0.0244361 \\ 0.0227522 & 0.0865821 & 0.0689065 \end{pmatrix}$$

Eq. 9.7

The matrix \mathbf{G} then became:

$$\mathbf{G} = \begin{pmatrix} 29.0177 & -14.5123 & -0.0079 \\ -14.5123 & 28.9444 & -0.0707 \\ -0.0079 & -0.0707 & 173.9730 \end{pmatrix}$$

Eq. 9.8

The \mathbf{G} matrix gave the cell dimensions; $a=5.3868$, $b=5.3800$, $c=13.1899$ Å, $\alpha=90.057$, $\beta=90.006$, $\gamma=120.050^\circ$. This cell looked apparently hexagonal, but actually it was not the TRUE triple hexagonal, i.e., the c_H is not the 'TRUE' three-fold axis. First of all, we found that this setting was 'reverse' by looking into the systematic conditions of reflections.

Therefore, we applied the conversion matrix from reverse to obverse using the transformation matrix \mathbf{U} as given in Eq. 2.1:

$$\mathbf{U} = \begin{pmatrix} -1 & 0 & 0 \\ 0 & -1 & 0 \\ 0 & 0 & 1 \end{pmatrix}$$

$$\mathbf{G}' = \mathbf{U}\mathbf{G}\mathbf{U}^T$$

$$\mathbf{G}' = \mathbf{G} = \begin{pmatrix} 29.0177 & -14.5123 & -0.0079 \\ -14.5123 & 28.9444 & -0.0707 \\ -0.0079 & -0.0707 & 173.9730 \end{pmatrix}$$

Eqs. 9.9

Further transformations were applied to the four possible rhombohedral cell models, \mathbf{R}_n ($n=1, 2, 3$, and 4), to obtain \mathbf{G}_n :

$$\mathbf{G}_n = \mathbf{P}_n\mathbf{G}_n\mathbf{P}_n^T$$

Eq. 9.10

$$\text{If } \mathbf{P}_1 = \begin{pmatrix} 2/3 & 1/3 & 1/3 \\ -1/3 & 1/3 & 1/3 \\ -1/3 & -2/3 & 1/3 \end{pmatrix}, \text{ then}$$

$$\mathbf{G}_1 = \begin{pmatrix} 28.9740 & 14.4690 & 14.5192 \\ 14.4690 & 28.9816 & 14.5196 \\ 14.5192 & 14.5196 & 29.0020 \end{pmatrix}$$

$$\text{If } \mathbf{P}_2 = \begin{pmatrix} -1 & -1 & 0 \\ 0 & -1 & 0 \\ -1/3 & -2/3 & 1/3 \end{pmatrix}, \text{ then}$$

$$\mathbf{G}_2 = \begin{pmatrix} 28.9376 & 14.4321 & 14.4304 \\ 14.4321 & 28.9444 & 14.4353 \\ 14.4304 & 14.4353 & 28.9356 \end{pmatrix}$$

$$\text{If } \mathbf{P}_3 = \begin{pmatrix} 1 & 0 & 0 \\ 1 & 1 & 0 \\ 2/3 & 1/3 & 1/3 \end{pmatrix}, \text{ then}$$

$$\mathbf{G}_3 = \begin{pmatrix} 29.0177 & 14.5054 & 14.5103 \\ 14.5054 & 28.9376 & 14.5072 \\ 14.5103 & 14.5072 & 29.0124 \end{pmatrix}$$

$$\text{If } \mathbf{P}_4 = \begin{pmatrix} 0 & 1 & 0 \\ -1 & 0 & 0 \\ -1/3 & 1/3 & 1/3 \end{pmatrix}, \text{ then}$$

$$\mathbf{G}_4 = \begin{pmatrix} 28.9444 & 14.5123 & 14.5091 \\ 14.5123 & 29.0177 & 14.5073 \\ 14.5091 & 14.5073 & 29.0095 \end{pmatrix}$$

Eqs. 9.11

The cell parameters obtained from the \mathbf{G}_n matrices are given in Table 9.1. The cell angles of the four candidates suggest that the TRUE cell is \mathbf{R}_2 with its 3-fold axis running parallel to $[-3, -6, 1]$ direction of the 'FALSE' triple-hexagonal (obverse) cell in Fig. 4.1.

9.3.2. Indirect conversion from the pseudo hexagonal to rhombohedral candidates via pseudo FCC cell

We can of course find a true cell through the route of pseudo FCC cell as described in Section 7. In this route we first transform the experimentally-obtained triple-hexagonal cell in reverse setting into obverse, and then transform the reverse into pseudo FCC. The four ‘rhombohedral’ cells with different orientations are then generated and given as R'_1, R'_2, R'_3, R'_4 in Table 9.2. Since we found a satisfactory result for the R'_3 , the cell was further transformed back into the triple-hexagonal obverse.

Comparing the rhombohedral models obtained

from the direct conversion from obverse to rhombohedral (Table 9.1) and from the indirect conversion *via* pseudo FCC (Table 9.2), we find a good agreement between $R_1 \leftrightarrow R'_1, R_2 \leftrightarrow R'_3, R_3 \leftrightarrow R'_2,$ and $R_4 \leftrightarrow R'_4$, respectively. No significant difference can be seen between these two routes except for the sequence of a, b, c, and some small truncation errors. This is because they are essentially the same procedures from mathematical point of view.

Table 9.1. Cell dimensions of the four ‘rhombohedral’ cells (R_2 in hatched line is the ‘TRUE’ cell).

cell	a	b	c	α	β	γ	comments
initial Hrev	5.3868	5.3800	13.1899	90.057	90.006	120.050	= R_1
R_1	5.3863	5.3860	5.3792	59.968	59.958	60.008	FALSE
R_2	5.3794	5.3800	5.3792	60.079	60.087	60.088	TRUE
R_3	5.3868	5.3794	5.3863	59.955	59.994	59.962	FALSE
R_4	5.3800	5.3868	5.386	59.999	59.953	59.950	FALSE
final Hobv	5.3868	5.3860	13.1686	89.992	90.010	120.001	from R_2

Table 9.2. Cell dimensions of the four ‘rhombohedral’ cells using an intermediate conversion into pseudo FCC cell. R'_3 in the hatched line is the TRUE rhombohedral cell.

	a	b	c	α	β	γ	comments
initial Hrev	5.3868	5.38	13.1899	90.057	90.006	120.05	= R'_1
FCC	7.6121	7.6134	7.6125	89.933	89.929	90.081	= R'_1
R'_1	5.3863	5.3860	5.3792	59.968	59.958	60.008	FALSE
R'_2	5.3794	5.3863	5.3868	59.994	59.962	59.955	FALSE
R'_3	5.3800	5.3794	5.3792	60.087	60.079	60.088	TRUE
R'_4	5.3860	5.3800	5.3868	59.95	59.999	59.953	FALSE
final Hobv ₃	5.3868	5.3863	13.1686	90.001	89.991	120.006	FALSE

10. Closing remarks

Discrimination between the rhombohedral and face-centred pseudo cubic unit cells is not difficult in principle, if we have fully accurate data about the cell dimensions. The accuracy of data is improving year by year through the various developments in experimentation, which favors the analysis of this kind. The repeated trials of this sort of discrimination on the Smart Apex II single-crystal diffractometer have suggested that we could distinguish the true rhombohedral cell orientation if the rhombohedral distortion angle of α departs more than 0.004° from 60° .

Acknowledgements

This work is supported by Grants-in-Aid for Scientific Research No. 18206071 from Japan So-

ciety of Promotion of Science. Part of the authors (YI) appreciates the Research Fellowship of the Japan Society for the Promotion of Science for Young Scientists. Synchrotron X-ray experiments were carried out at KEK-PF under the programs, No. 2007G027 and 2007G028.

References

- [1] International Tables for Crystallography Vol. A, p84 (2002).
- [2] H. D. Megow, ‘Crystal Structures: A Working Approach’, W.B. Saunders Company, Philadelphia (1973).
- [3] P. Niggli, ‘Handbuch der Experimentalphysik, Vol.7, Part 1’, Leipzig: Akademische Verlagsgesellschaft, (1928).

Appendix 1. Relation between the c/a ratio for the triple-hexagonal cell and the interaxial angle α in degree for the primitive rhombohedral cell. Data line at $\alpha=60^\circ$ and $c/a=\sqrt{6}$ is hatched.

α	c/a	α	c/a	α	c/a	α	c/a	α	c/a
59.700	2.4662	59.820	2.4595	59.940	2.4528	60.060	2.4461	60.180	2.4395
59.702	2.4661	59.822	2.4594	59.942	2.4527	60.062	2.4460	60.182	2.4394
59.704	2.4660	59.824	2.4592	59.944	2.4526	60.064	2.4459	60.184	2.4393
59.706	2.4658	59.826	2.4591	59.946	2.4524	60.066	2.4458	60.186	2.4391
59.708	2.4657	59.828	2.4590	59.948	2.4523	60.068	2.4457	60.188	2.4390
59.710	2.4656	59.830	2.4589	59.950	2.4522	60.070	2.4456	60.190	2.4389
59.712	2.4655	59.832	2.4588	59.952	2.4521	60.072	2.4455	60.192	2.4388
59.714	2.4654	59.834	2.4587	59.954	2.4520	60.074	2.4453	60.194	2.4387
59.716	2.4653	59.836	2.4586	59.956	2.4519	60.076	2.4452	60.196	2.4386
59.718	2.4652	59.838	2.4585	59.958	2.4518	60.078	2.4451	60.198	2.4385
59.720	2.4651	59.840	2.4584	59.960	2.4517	60.080	2.4450	60.200	2.4384
59.722	2.4649	59.842	2.4582	59.962	2.4516	60.082	2.4449	60.202	2.4383
59.724	2.4648	59.844	2.4581	59.964	2.4514	60.084	2.4448	60.204	2.4381
59.726	2.4647	59.846	2.4580	59.966	2.4513	60.086	2.4447	60.206	2.4380
59.728	2.4646	59.848	2.4579	59.968	2.4512	60.088	2.4446	60.208	2.4379
59.730	2.4645	59.850	2.4578	59.970	2.4511	60.090	2.4445	60.210	2.4378
59.732	2.4644	59.852	2.4577	59.972	2.4510	60.092	2.4443	60.212	2.4377
59.734	2.4643	59.854	2.4576	59.974	2.4509	60.094	2.4442	60.214	2.4376
59.736	2.4642	59.856	2.4575	59.976	2.4508	60.096	2.4441	60.216	2.4375
59.738	2.4640	59.858	2.4573	59.978	2.4507	60.098	2.4440	60.218	2.4374
59.740	2.4639	59.860	2.4572	59.980	2.4506	60.100	2.4439	60.220	2.4373
59.742	2.4638	59.862	2.4571	59.982	2.4504	60.102	2.4438	60.222	2.4372
59.744	2.4637	59.864	2.4570	59.984	2.4503	60.104	2.4437	60.224	2.4370
59.746	2.4636	59.866	2.4569	59.986	2.4502	60.106	2.4436	60.226	2.4369
59.748	2.4635	59.868	2.4568	59.988	2.4501	60.108	2.4435	60.228	2.4368
59.750	2.4634	59.870	2.4567	59.990	2.4500	60.110	2.4433	60.230	2.4367
59.752	2.4633	59.872	2.4566	59.992	2.4499	60.112	2.4432	60.232	2.4366
59.754	2.4632	59.874	2.4565	59.994	2.4498	60.114	2.4431	60.234	2.4365
59.756	2.4630	59.876	2.4563	59.996	2.4497	60.116	2.4430	60.236	2.4364
59.758	2.4629	59.878	2.4562	59.998	2.4496	60.118	2.4429	60.238	2.4363
59.760	2.4628	59.880	2.4561	60.000	2.4494	60.120	2.4428	60.240	2.4362
59.762	2.4627	59.882	2.4560	60.002	2.4493	60.122	2.4427	60.242	2.4360
59.764	2.4626	59.884	2.4559	60.004	2.4492	60.124	2.4426	60.244	2.4359
59.766	2.4625	59.886	2.4558	60.006	2.4491	60.126	2.4425	60.246	2.4358
59.768	2.4624	59.888	2.4557	60.008	2.4490	60.128	2.4423	60.248	2.4357
59.770	2.4623	59.890	2.4556	60.010	2.4489	60.130	2.4422	60.250	2.4356
59.772	2.4621	59.892	2.4555	60.012	2.4488	60.132	2.4421	60.252	2.4355
59.774	2.4620	59.894	2.4553	60.014	2.4487	60.134	2.4420	60.254	2.4354
59.776	2.4619	59.896	2.4552	60.016	2.4486	60.136	2.4419	60.256	2.4353
59.778	2.4618	59.898	2.4551	60.018	2.4484	60.138	2.4418	60.258	2.4352
59.780	2.4617	59.900	2.4550	60.020	2.4483	60.140	2.4417	60.260	2.4351
59.782	2.4616	59.902	2.4549	60.022	2.4482	60.142	2.4416	60.262	2.4349
59.784	2.4615	59.904	2.4548	60.024	2.4481	60.144	2.4415	60.264	2.4348
59.786	2.4614	59.906	2.4547	60.026	2.4480	60.146	2.4414	60.266	2.4347
59.788	2.4613	59.908	2.4546	60.028	2.4479	60.148	2.4412	60.268	2.4346
59.790	2.4611	59.910	2.4544	60.030	2.4478	60.150	2.4411	60.270	2.4345
59.792	2.4610	59.912	2.4543	60.032	2.4477	60.152	2.4410	60.272	2.4344
59.794	2.4609	59.914	2.4542	60.034	2.4476	60.154	2.4409	60.274	2.4343
59.796	2.4608	59.916	2.4541	60.036	2.4474	60.156	2.4408	60.276	2.4342
59.798	2.4607	59.918	2.4540	60.038	2.4473	60.158	2.4407	60.278	2.4341
59.800	2.4606	59.920	2.4539	60.040	2.4472	60.160	2.4406	60.280	2.4340
59.802	2.4605	59.922	2.4538	60.042	2.4471	60.162	2.4405	60.282	2.4338
59.804	2.4604	59.924	2.4537	60.044	2.4470	60.164	2.4404	60.284	2.4337
59.806	2.4602	59.926	2.4536	60.046	2.4469	60.166	2.4402	60.286	2.4336
59.808	2.4601	59.928	2.4534	60.048	2.4468	60.168	2.4401	60.288	2.4335
59.810	2.4600	59.930	2.4533	60.050	2.4467	60.170	2.4400	60.290	2.4334
59.812	2.4599	59.932	2.4532	60.052	2.4466	60.172	2.4399	60.292	2.4333
59.814	2.4598	59.934	2.4531	60.054	2.4464	60.174	2.4398	60.294	2.4332
59.816	2.4597	59.936	2.4530	60.056	2.4463	60.176	2.4397	60.296	2.4331
59.818	2.4596	59.938	2.4529	60.058	2.4462	60.178	2.4396	60.298	2.4330

Appendix 2. Selected reflections indexed by the pseudo FCC, rhombohedral, and triple-hexagonal obverse. $N=h^2+k^2+l^2$, $i=-h-k$. The equivalent reflection groups are hatched with the same tone. The reflection conditions for $R\bar{3}c$ groups are indicated ('x' stands for extinct). All reflection appears in $R\bar{3}$.

N	pseudo FCC			R			Hobv				$R\bar{3}c$	
	<i>h</i>	<i>k</i>	<i>l</i>	<i>h</i>	<i>k</i>	<i>l</i>	<i>h</i>	<i>k</i>	<i>i</i>	<i>l</i>		
3	1	1	1	1	1	1	0	0	0	3	x	
	-1	1	1	1	0	0	1	0	-1	1	x	
	1	-1	1	0	1	0	-1	1	0	1	x	
	1	1	-1	0	0	1	0	-1	1	1	x	
4	2	0	0	0	1	1	-1	0	1	2	○	
	0	2	0	1	0	1	1	-1	0	2	○	
	0	0	2	1	1	0	0	1	-1	2	○	
8	0	2	2	2	1	1	1	0	-1	4	○	
	2	0	2	1	2	1	-1	1	0	4	○	
	2	2	0	1	1	2	0	-1	1	4	○	
	0	-2	2	0	1	-1	-1	2	-1	0	○	
	2	0	-2	-1	0	1	-1	-1	2	0	○	
	-2	2	0	1	-1	0	2	-1	-1	0	○	
11	3	1	1	1	2	2	-1	0	1	5	x	
	1	3	1	2	1	2	1	-1	0	5	x	
	1	1	3	2	2	1	0	1	-1	5	x	
	3	-1	-1	-1	1	1	-2	0	2	1	x	
	-1	3	-1	1	-1	1	2	-2	0	1	x	
	-1	-1	3	1	1	-1	0	2	-2	1	x	
	3	1	-1	0	1	2	-1	-1	2	3	○	
	-1	3	1	2	0	1	2	-1	-1	3	○	
	1	-1	3	1	2	0	-1	2	-1	3	○	
	3	-1	1	0	2	1	-2	1	1	3	○	
	1	3	-1	1	0	2	1	-2	1	3	○	
	-1	1	3	2	1	0	1	1	-2	3	○	
12	2	2	2	2	2	2	0	0	0	6	○	
	-2	2	2	2	0	0	2	0	-2	2	○	
	2	-2	2	0	2	0	-2	2	0	2	○	
	2	2	-2	0	0	2	0	-2	2	2	○	
	19	1	-3	3	0	2	-1	-2	3	-1	1	○
		3	1	-3	-1	0	2	-1	-2	3	1	○
		-3	3	1	2	0	-1	3	-1	-2	1	○
		1	3	-3	0	-1	2	1	-3	2	1	○
		-3	1	3	2	0	-1	2	1	-3	1	○
		3	-3	1	-1	2	0	-3	2	1	1	○
		1	3	3	3	2	2	1	0	-1	7	x
		3	1	3	2	3	2	-1	1	0	7	x
		3	3	1	2	2	3	0	-1	1	7	x
		1	-3	-3	-3	-1	-1	-2	0	2	-5	x
		-3	1	-3	-1	-3	-1	2	-2	0	-5	x
		-3	-3	1	-1	-1	-3	0	2	-2	-5	x
35		5	3	1	2	3	4	-1	-1	2	9	○
		1	5	3	4	2	3	2	-1	-1	9	○
		3	1	5	3	4	2	-1	2	-1	9	○
		5	1	3	2	4	3	-2	1	1	9	○
	3	5	1	3	2	4	1	-2	1	9	○	
	1	3	5	4	3	2	1	1	-2	9	○	
	5	3	-1	1	2	4	-1	-2	3	7	○	
	-1	5	3	4	1	2	3	-1	-2	7	○	
	3	-1	5	2	4	1	-2	3	-1	7	○	
	5	-1	3	1	4	2	-3	2	1	7	○	
	3	5	-1	2	1	4	1	-3	2	7	○	
	-1	3	5	4	2	1	2	1	-3	7	○	
	5	-3	-1	-2	2	1	-4	1	3	1	○	
	-1	5	-3	1	-2	2	3	-4	1	1	○	
	-3	-1	5	2	1	-2	1	3	-4	1	○	
	5	-1	-3	-2	1	2	-3	-1	4	1	○	
-3	5	-1	2	-2	1	4	-3	-1	1	○		
-1	-3	5	1	2	-2	-1	4	-3	1	○		
5	-3	1	-1	3	1	-4	2	2	3	○		
1	5	-3	1	-1	3	2	-4	2	3	○		
-3	1	5	3	1	-1	2	2	-4	3	○		
-5	3	-1	1	-3	-1	4	-2	-2	-3	○		
-1	-5	3	-1	1	-3	-2	4	-2	-3	○		
3	-1	-5	-3	-1	1	-2	-2	4	-3	○		